Bioresource Technology 110 (2012) 595–602

Contents lists available at SciVerse ScienceDirect

Bioresource Technology

journal homepage: www.elsevier.com/locate/biortech

Combustion behaviours of tobacco stem in a thermogravimetric analyser and a pilot-scale fluidized bed reactor

Zixu Yang [a], Shihong Zhang [a,*], Lei Liu [a,b], Xiangpeng Li [a], Hanping Chen [a], Haiping Yang [a], Xianhua Wang [a]

[a] *State Key Laboratory of Coal Combustion, Huazhong University of Science and Technology, Wuhan, Hubei 430074, PR China*
[b] *Hubei Research and Design Institute of Chemical Industry, PR China*

ARTICLE INFO

Article history:
Received 8 October 2011
Received in revised form 22 December 2011
Accepted 22 December 2011
Available online 12 January 2012

Keywords:
Tobacco stem
Thermogravimetric analysis
Fluidized bed combustion
Agglomeration

ABSTRACT

Despite its abundant supply, tobacco stem has not been exploited as an energy source in large scale. This study investigates the combustion behaviours of tobacco stem in a thermogravimetric analyser (TGA) and a pilot-scale fluidized bed (FB). Combustion characteristics, including ignition and burnout index, and combustion reaction kinetics were studied. Experiments in the FB investigated the effects of different operating conditions, such as primary air flow, secondary air flow and feeding rates, on the bed temperature profiles and combustion efficiency. Two kinds of bed materials cinder and silica sand were used in FB and the effect of bed materials on agglomeration was studied. The results indicated that tobacco stem combustion worked well in the FB. When operation condition was properly set, the tobacco stem combustion efficiency reached 94%. In addition, compared to silica sand, cinder could inhibit agglomeration during combustion because of its high aluminium content.

1. Introduction

The supply of tobacco waste is abundant but there is no effective way to treat or exploit the materials. In China, tobacco production and curing is ranked among the most important agro-industries, involving hundreds of millions of farmers and workers and, thus, contributing significantly to the national economy. However, the tobacco manufacturing process consumes considerable amounts of energy but with little efficiency. According to (Xu et al., 2000), the average energy cost involved in tobacco curing is 2.2–3.2 kg of standard coal for per 1 kg of tobacco, with a process energy efficiency of less than 20%. In addition, a large amount of energy is dissipated through incomplete combustion, flue gas emission and heat transfer, and the energy cost is then significantly increased. Furthermore, this considerable use of fossil fuels can harm the environment through air pollution, greenhouse gas, acid rain and so on (Quadrelli and Peterson, 2007). Therefore, a potential solution is essential to address all of the issues mentioned above. It has been reported that the production of approximately 5 million tons of dried tobacco (Li et al., 2010) yields 1 million tons of tobacco waste. If such large amount of tobacco waste could possibly be utilized to provide energy for the tobacco curing in an effective and clean method, it would satisfy the objectives of both energy conservation and environmental protection.

Tobacco waste is a typical agricultural waste material produced during the manufacturing of tobacco. The range of waste products generated from tobacco is diverse, and mainly includes tobacco stems, tobacco dust and tobacco residue (Piotrowska-Cyplik et al., 2009; Zhong et al., 2010). Large amount of tobacco waste is generated every year, and the disposal of the waste has generated widespread concern in the tobacco industry because of their high content of toxic chemicals, such as nicotine, which is harm to both the environment and human health (Barrena et al., 2008). However, these large yields of tobacco waste could provide a new fuel resource if used appropriately. The conventional methods for disposal for tobacco waste, including burning it in stacks and dumping in landfills, not only result in serious environmental pollution but also cause wastage of resources. Novel approaches proposed for the use of tobacco stem mainly include: (1) extraction of nicotine and nicotinic acid (Lu, 2000); (2) preparation of activated carbon (Li et al., 2008); (3) manufacturing of fibre board (Castron and Agrupis, 2000). In addition, many researchers have studied the thermochemical conversion of tobacco waste as a means of alternative energy production. For instance, Valverde et al. (2000) studied the pyrolysis kinetics of tobacco dust in a TGA under different heating rates and established a model for volatile evolution. Sung and Seo (2009) studied the non-isothermal behaviour of two different types of tobacco stem on a TGA and concluded that the conditions of decomposition and type of tobacco variety used were the major factors contributing to the weight-loss patterns. Li et al. (2011) investigated the co-combustion characteristics of tobacco residue and high-ash anthracite coal on TGA under different temperatures in

---

* Corresponding author. Tel.: +86 3307107197; fax: +86 27 87545526.
E-mail address: shzhang@hust.edu.cn (S. Zhang).

0960-8524/$ - see front matter © 2012 Published by Elsevier Ltd.
doi:10.1016/j.biortech.2011.12.119

mixed proportion and reported that co-combustion improved the combustion characteristics when compared with the separate burning of tobacco residue and coal, particularly with regard to the ignition and burnout characteristics; they proposed a method that could enable their use as an alternative fuel source. Unfortunately, most of these technologies developed for disposal of tobacco waste disposal have not been widely applied commercially because of limitations of low disposing capabilities, high cost and complex processes. Therefore, identification of suitable methods for efficient and cost-effective disposal of tobacco wastes is of significant importance.

Fluidized bed (FB) is a proven technology that has been applied commercially for clean combustion of fossil fuels and biomass because of its excellent fuel flexibility, high heat and mass transfer efficiency and low operating temperature and toxic gas emission (Kouprianov and Permchart, 2003). Numerous studies of biomass combustion on the FB have been reported (Andreae, 1991; Li et al., 2009). However, biomass has several drawbacks such as low bulk density and low heating value, high moisture and alkali metal concentrations, different chemical compositions and feeding difficulties(Gil et al., 2010b; Gogebakan et al., 2009), Therefore, suitable further research work is required to identify methods to resolve these problems and to improve its combustion characteristics.

This study aimed to assess the fuel characteristics of tobacco stem with regard to TGA and FB facilities. To provide a better understanding of the combustion of tobacco stems in FB, experimental results of temperature profiles and stack gas composition during the combustion process have been presented and discussed. Furthermore, the phenomenon of bed material agglomeration during combustion was investigated and analysed, and a suitable alternative bed material has been proposed. The results discussed in this article may provide theoretical support for significantly efficient utilization of tobacco stem in the tobacco manufacturing industry.

2. Methods

2.1. Materials

2.1.1. Properties of tobacco stem

Tobacco stem is the residue generated during the harvesting of tobacco leaf; the stem has a rigid structure composed of sclerenchyma and cell-wall biopolymers such as cellulose, the contents of which vary depending on the characteristics of soil, climate, the environment and the varieties of tobacco plants. In addition, the tobacco stem is susceptible to moisture and degrades with humidity, making it difficult to store and transport.

In the present study, tobacco stems obtained from Enshi, in Hubei Province of China, were crushed to obtain stems that were 5–10 cm in length and approximately 1 cm wide. Tobacco stems are very light, with a packing density in the range of 289–321 kg/m^3 and true density of approximately 1657 kg/m^3. Proximate analyses of tobacco stem were conducted in accordance with standards prescribed by the American Society for Testing and Materials (ASTM) to obtain details of moisture content, volatile components and fixed carbon and ash content. Ultimate analyses of dried samples for carbon, hydrogen, nitrogen and sulphur composition were carried out with a CHNS/O elementary analyser (Vario Micro cube, Germany). The low gross calorific values of the dried samples were measured by bomb calorimeter (Parr 6300, USA). Results of the analysis of tobacco stem are provided in Table 1, suggesting that the tobacco stem has a high volatile and ash content and low gross calorific value of 11.3 MJ/kg. The molecular formula of $C_{2.722}H_{5.66}O_{1.994}N_{0.2721}S_{0.0238}$ was obtained based on the ultimate analysis of tobacco stem by dividing the content of C, H, O, N, and S by their relative atomic mass.

2.1.2. Characteristics of bed materials

In this study, two types of bed materials, silica sand and cinder, were studied. Many studies have reported that silica sand is more likely to lead bed agglomeration in FB during biomass combustion because of its high content of SiO_2 (Barrena et al., 2008; Bartels et al., 2008). For comparison, the cinder was used as an alternative bed material because of its ability to diminish agglomeration and accessibility (Brus et al., 2004). Both the silica sand and cinder were pelletized to 0.1–1 mm and 1–2 mm particles, respectively. In addition, the fluidization of bed materials was examined in a cold test mode facility, and the minimum fluidized velocity for silica sand and cinder was determined as 0.20 and 0.45 m/s, respectively.

2.2. Experiments on TGA

2.2.1. Apparatus and experimental conditions

First, the samples were sieved to obtain a particle size of less than 0.2 mm and, then, dehydrated in air at temperatures lower than 105 °C. The experiment was carried out on a STA-409C Thermal Analyser (NETZSCH Corp., Germany). The thermal analysis was carried out at atmospheric pressure with an air flow rate of 60 ml/min at a heating rate of 20 °C/min from room temperature to 800 °C. Approximately 16 mg of sample was used for the experiment. In this test, the sample mass ranging from 10 to 20 mg was proved to have no significant impact on combustion of tobacco stem, which was consistent with findings from (Yang et al., 2004). The weight loss (TG curve) and derivative weight loss (DTG curve) of the sample were represented as a function of temperature and time.

2.2.2. Ignition and burnout index

The ignition temperature T_i reflects the difficulty in the ignition of fuel, which is related to the difficulty in inducing a combustion reaction; a lower ignition temperature indicates a favourable reaction activity of the fuel. In the present study, the ignition index D_i and the burnout index D_f were used to describe the ignition and burnout characteristics of tobacco stem (Hurt and Gibbins, 1995):

$$D_i = \frac{DTG_{\max}}{t_p t_i} \tag{1}$$

$$D_f = \frac{DTG_{\max}}{\Delta t_{1/2} t_p t_f} \tag{2}$$

where $DTG_{\max}$ (%/min) denotes the maximum combustion rate; t_p (min) is the corresponding time of the maximum combustion rate; $\Delta t_{1/2}$ (min) represents the time range that corresponds to $DTG/DTG_{\max} = 1/2$; and t_i (min) and t_f (min) represent the ignition time and burnout time, respectively.

2.2.3. Combustion reaction kinetics

The combustion process is assumed to be composed of simple thermochemical reactions, and the relative combustion kinetics index was calculated by the Coats–Redfern method, as used by other researchers (Varhegyi et al., 1997):

$$\ln[F(\alpha)] = -(E/RT) + \ln(AR/\beta E) \tag{3}$$

$$F(\alpha) = -\ln(1-\alpha)/T^2 \quad (\text{for } n = 1) \tag{4}$$

$$F(\alpha) = [1-(1-\alpha)^{1-n}]/(1-n)T^2 \quad (\text{for } n \neq 1) \tag{5}$$

where, α represents the conversion rate of biomass fuels, which is defined as $\alpha = (\omega_0 - \omega)/(\omega_0 - \omega_\infty)$, ω is the sample weight at time t, ω_0 and ω_∞ denote the initial and final weights of the sample, respectively, β is the heating rate, n is defined as the order of the reaction, E and A represent the reaction energy and pre-exponential frequency factor and R is the ideal gas constant ($R = 8.314$ J/mol/K).

Table 1
Ultimate and proximate analyses of tobacco stem analysis.

Proximate analysis (wt.%)					Ultimate analysis (wt.%)					LHV(MJ/kg)
M_{ar}	M_{ad}	V_{ad}	A_{ad}	FC_{ad}	C_{ad}	H_{ad}	O_{ad}	N_{ad}	S_{ad}	Q_{ad}
20.86	3.51	68.64	21.70	6.14	32.66	5.66	31.91	3.81	0.76	11.30

Note: M_{ar}, Moisture (received basis); M_{ad}, Moisture (air dried basis); V_{ad}, Volatile Matter (air dried basis); A_{ad}, Ash (air dried basis); FC_{ad}, Fixed-Carbon (air dried basis); Q_{ad}, Low Heating Value (air dried basis).

Multiple reaction orders were assumed for the combustion reaction, and the optimum reaction order was determined when the plot of $\ln[F(\alpha)]$ versus $-1/T$ is a straight line, and then the activation energy E and pre-exponential frequency factor A can be obtained from the slope and intercept of the line, respectively.

2.3. Experiments on FB

2.3.1. FB facility

The apparatus used for tobacco stem combustion is schematically shown in Fig. 1. The system comprises a combustor, an under-bed hot-air ignition system, a wind box, an air distributor and a fly-ash separating system (composed of a downward exhausting cyclone and a loop seal), a grated water/air cooling system and a flue gas cleaning system. The biomass feeding system is composed of a bin and a screw feeder, and the feeding rate of the tobacco stem is determined by the rotational speed of the screw feeder, which is controlled by a motor. In the tests, the feeder system could operate continuously and the feeding rate could be adjusted flexibly.

The FB column has an overall height of 10 m and consists of a dense phase zone of 108 mm and a dilute phase zone of 150 mm in inner diameter. The entrance for the secondary air is located 1720 mm above the air distributor. A peep port and a sampling port are located along the column to facilitate observation of the burning conditions and sample collection, respectively. The temperature distribution along the column was continuously measured by nine thermocouples of type K (T1–T9). The pressure drop between the wind-box and burning region was measured by U-tube water manometers. The significant fluctuation in pressure drop in the bed indicates the increasing likelihood of defluidization.

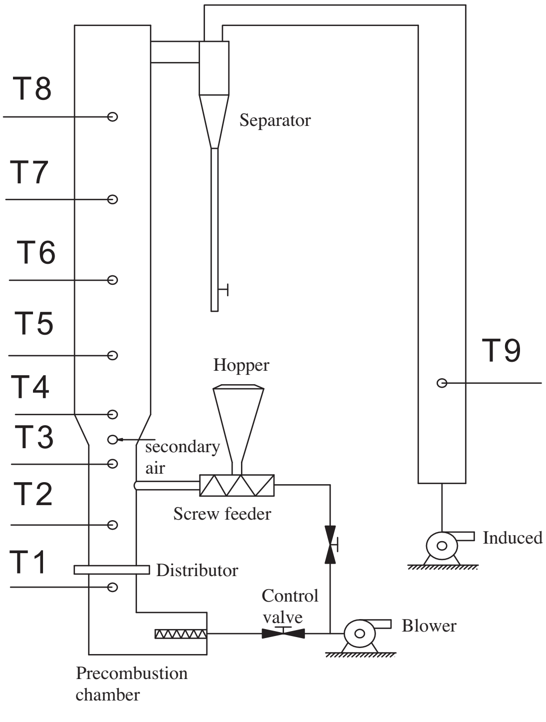

Fig. 1. Schematic diagram of the FB test facility.

2.3.2. Experimental methods

The bed materials were fed into the combustor, before the experiment, with a static bed height of 200 mm. At the beginning of the experiment, the combustor was preheated with coal gas. The ignition temperature of tobacco stem is determined from the TG analysis above, which is about 250 °C. Therefore, when the temperature of the dense phase zone reached a temperature higher than this, the gas supply was reduced gradually and the tobacco stem was fed into the combustor manually. As the temperature in the dense phase zone reached 600 °C, the coal gas supply was cut off and the tobacco stem was fed into the combustor continuously at a rate of between 8 and 12 kg/h. The temperatures at different heights of the bed were monitored simultaneously. The primary air and secondary air flows were controlled by adjusting the flowmeter controllers. And the temperature distribution along the bed height and pressure drop between wind-box and boiling zone were monitored online. A Fourier Transform Infrared (FTIR) Gas Analyser (GASMET DX400) and a hand-held gas analyser (Kane KM940) were used to measure the concentrations of O_2, CO_2, NO, SO_2 and CH_4 in the stack gas. The air equivalent ratio (ER) is defined as follows:

$$ER = \frac{Q_{Total}}{\dot{M} \times V^0} \tag{6}$$

where Q_{Total} (m^3/h) represents the amount of total air flow into the combustor, $\dot{M}$ (kg/h) represents the feeding rate of the fuel, V^0(m^3) is the theoretical air consumption for complete combustion of per 1 kg of fuel.

The complete combustion at ER = 1 can be described as follows:

$$\begin{aligned} & C_{2.722}H_{5.66}O_{1.994}N_{0.2721}S_{0.0238} + 3.43590_2 + 12.925N_2 \\ & \quad + 1.095H_2O + ash \\ & \quad = 2.722CO_2 + 3.925H_2O + 12.925N_2 + 0.2721NO_2 \\ & \qquad + 0.0238SO_2 \end{aligned} \tag{7}$$

It is assumed that the input fuel to the combustor was composed of combustibles, moisture and ash, and the water content on the left side of the equation was determined by the initial moisture content from proximate analysis. Therefore, this equation provides a theoretical foundation for the possible gaseous emissions during combustion.

The fluidized velocity was derived by dividing the primary air flow by the cross-sectional area of dense phase zone in the combustor. In this experiment, the ER was set at 1.1–1.30, and the fluidized velocity was set in the range 0.40–0.57 m/s.

This series of experiments were conducted to observe the bed temperature profiles under different flow rates of primary air, secondary air and the agglomeration characteristics of two types of bed materials in the FB. The experiment was forcibly terminated when a high temperature or significant fluctuation in pressure drop was observed, which indicated the occurrence of bed agglomeration.

3. Results and discussions

3.1. Thermal behaviour of tobacco stems

The combustion pattern of the tobacco stem sample is shown in Fig. 2. The weight loss below 185 °C was due to the evaporation of the moisture content retained in the sample, which accounted for approximately 5% of the weight loss (Valverde et al., 2000). The decomposition during combustion mainly occurred in the temperature range 185–410 °C, and two peaks were observed in this range. Facilitated by the rapid combustion of volatile components, the peak around 300 °C occurred due to the thermal decomposition of cell-wall biopolymers such as cellulose, hemicellulose, and so on (Wang et al., 2005). In addition, the peak around 390 °C occurred due to the carbonization of lignin and combustion of char residue. The combustion was maintained at a lower rate because of the decline in the rate of cellulose decomposition (Sung and Seo, 2009). The third peak around 540 °C originated from the further oxidation of the char residue.

The ignition and burnout temperatures were determined by adopting an extrapolation method (Li et al., 2011; Wang et al., 2009) in TG and DTG curves. The indices describing the characteristics of ignition and burnout are listed in Table 2.

The combustion characteristics of different fuels varied because of their various chemical compositions. In general, combustion reaction consists of two stages (Gil et al., 2010a):

$$\mathrm{A(fuel)} \rightarrow \mathrm{B(char)} + \mathrm{C1(gas)(stage\ 1)}$$

$$\mathrm{B(char)} + \mathrm{O_2} \rightarrow \mathrm{C2(gas)} + \mathrm{D(ash)(stage\ 2)}$$

For most biomass fuels, the volatile matters are the main components, which accounts for most of the weight loss at lower temperatures, and thus leads to a lower ignition temperature. In addition, the release patterns of volatile matters in different biomass substances change according to their chemical composition. In a study by Wang et al. (2009), the ignition temperatures of sawdust and wheat straw were 279 and 262 °C, respectively, both of which are higher than that of tobacco stem. The possible reason for this variation is differences in contents of cellulose, hemicellulose and lignin. Since, tobacco stem is rich in cellulose, it easily decomposes at lower temperatures; since the other two samples are abundant in lignin, they were more stable at lower temperatures. Therefore, more heat is needed to enhance the devolatilization process, and the ignition temperature increases as a result.

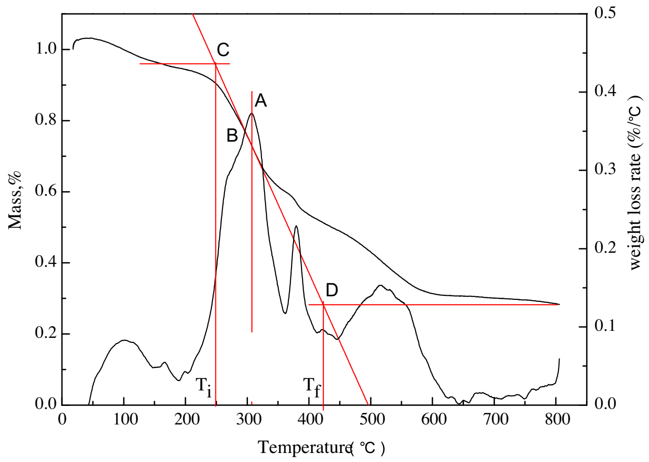

Fig. 2. Ignition temperature of tobacco stem in TG&DTG curves.

Activation energy and pre-exponential factors were used to estimate the difficulty and intensity of combustion reaction for tobacco stems and other two typical biomass fuels, under the same experimental conditions, as shown in Table 3. The combustion of tobacco stems comprises three different stages of mass loss after the loss of moisture, whereas no apparent transition stage has been observed in the other two biomass fuels mentioned above. It is evident from Table 3 that Activation energy E and Pre-exponential factor A for tobacco stem are low in the devolatilization stage, which indicates that it is easy to burn. In addition, the higher values of Activation energy E and Pre-exponential factor A in the transition stage indicate that the combustion reaction takes place at a very slow rate mainly because the combustion of gaseous volatiles has almost completed and lignin begins to carbonize at this stage. Tobacco stem has the lowest weight-loss percentage in the devolatilization region and the highest weight-loss percentage in the char residue combustion region, which indicates that the combustion reaction is dominated by burning of char.

3.2. Combustion characteristics of tobacco stem on FB

In this study, the influence of various operating conditions including feeding rate, primary and second air flow rate, air split ratio on the combustion efficiency and bed temperature were investigated. Data from seven different runs were recorded for discussion, and the relative operating parameters and results are summarized in Table 4. The combustion efficiency at different runs can be calculated according to the CO and CO_2 emission in stack gas and unburned carbon in fly ash. When burning tobacco stem in the FB, the unburned carbon collected in fly ash and bed material was quite limited; therefore, the combustion efficiency (η) is mainly determined by the concentration of CO and CO_2 in stack gas as follows:

$$\eta = \frac{\mathrm{CO_2}[\%]}{\mathrm{CO}[\%] + \mathrm{CO_2}[\%]} \tag{8}$$

3.2.1. Effect of primary air on the temperature distribution in the combustor

The bed temperature profile is shown in Fig. 3 under various flow rates of primary air when the feeding rate and the flow rate of secondary air were fixed at 8 kg/h and 17 m^3/h, respectively. As shown in Fig. 3, the temperature increased along the bed height and attained a maximum value in the range of 870–900 °C at the location of the feeding point and secondary air, and then decreased. According to the TGA analysis described above, large amounts of gaseous volatiles evolved from the tobacco stem at temperatures between 200 and 350 °C, and most of the heat was generated by the combustion of these gaseous volatiles. Thus, the observed temperature peak was attributed to the rapid release and combustion of volatiles at the feeding point. Similar results have been reported in the literature (Chirone et al., 2008; Tarelho et al., 2011). As the flow rate of primary air increased from 14 m^3/h to 16 m^3/h, the highest temperature in the dense-phase zone dropped drastically and the dilute-phase temperature increased and then decreased gradually. This phenomenon could be explained as follows: the overall heat input into the combustor is constant because of the fixed feeding rate. The increase of primary air enhances the mixing and disturbance of air and supplies adequate oxygen. The heat generated by the combustion of volatiles is brought up to the upper region of the combustor, and the combustion intensity zone is extended to the dilute phase zone gradually, resulting in a uniform temperature distribution there. However, in this experiment, there exists obvious temperature gradient along the combustor. One possible reason is that low primary

Table 2
Ignition and burnout index of tobacco stem.

Combustion parameters					Ignition index		Burnout index	
DTG_{max} (%/min)	t_p (min)	t_i (min)	t_f (min)	$\Delta t_{1/2}$ (min)	T_i (°C)	D_i ($\times 10^{-3}$)	D_f ($\times 10^{-4}$)	T_f (°C)
7.46	13.4	10.5	19.5	2.85	250	53.021	100.17	430

Note: DTG_{max}, maximum combustion rate; t_p, corresponding time of the maximum combustion rate; t_i, ignition time; t_f, burnout time; $\Delta t_{1/2}$, time range of $DTG/DTG_{max} = 1/2$; T_i, ignition temperature; T_f, burnout temperature; D_i, ignition index; D_f, burnout index.

Table 3
Combustion reaction kinetics results for different biomass samples.

Samples	Temperature range (°C)	Weight loss (%)	n	E (kJ/mol)	A (S^{-1})	R
Wheat straw	220–335	74.18	1	79.06	5.39E+13	0.9663
	335–501	13.01	3	124.27	3.22E+5	0.9898
Cotton straw	226–364	63.75	1	109.62	3.94E+7	0.9931
	364–446	25.46	3	257.04	7.25E+17	0.9761
Tobacco stem	220–350	33.00	1	91.60	1.09E+8	0.9953
	350–450	11.29	3	394.43	5.74E+26	0.9940
	450–620	30.92	2	291.14	1.35E+19	0.9631

Note: n, reaction order; E, reaction activation energy; A, pre-exponential frequency factor; R, correlation coefficient.

Table 4
Conditions of tobacco stem combustion.

Runs	Feeding rate (kg/h)	ER	$Q_{Primary}$ (Nm^3/h)	$Q_{Secondary}$ (Nm^3/h)	$Q_{primary}/Q_{secondary}$	O_2 (%)	CO (%)	CO_2 (%)	η
1	4.5	1.05	14	0	∞	5.1	1.59	14.1	0.8987
2	8	1.09	14	10	1:0.71	7.4	1.08	11.9	0.9168
3	8	1.18	14	12	1:0.86	4.9	2.32	14.2	0.8596
4	9	1.29	16	16	1:1	6.5	2.11	12.8	0.8584
5	10	1.12	14	17	1:1.21	7.6	0.88	12.0	0.9317
6	10	1.20	14	19	1:1.36	5.8	0.85	13.4	0.9404
7	12	1.06	19	16	1:0.84	5.3	1.36	12.5	0.9019

Note: $Q_{primary}$, the flow rate of primary air; $Q_{secondary}$, the flow rate of secondary air; η, combustion efficiency.

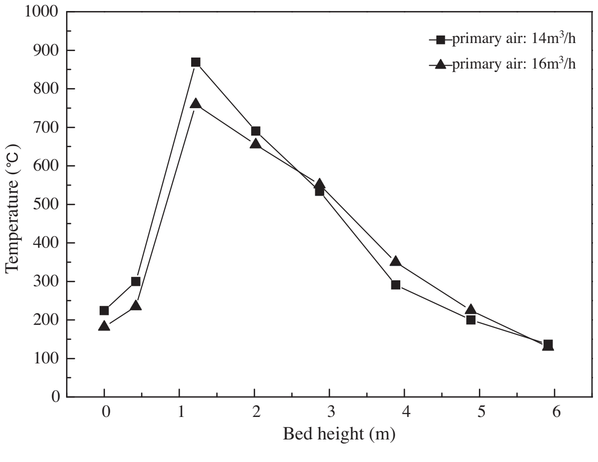

Fig. 3. The effect of primary air on the bed temperature profiles.

air flow leads to the inadequate mixing and disturbance of air and fuel. If the combustor is operated at a higher primary air flow, the combustion section will stretch to the top of the combustor and reduce the emission of unburned combustibles. However, the residence time of particles will decrease when excessive primary air is added, resulting in an increase of combustibles in flue gas and the loss of combustion efficiency (Fang et al., 2004). Therefore, there exists an optimum value for the primary air flow.

3.2.2. Effect of secondary air flow rate on the temperature distribution in the combustor

The secondary air plays an important role in promoting the combustion efficiency and reducing the emission of toxic pollutants. Basically, the secondary air supplements the oxygen supply required to burn the volatiles released from the dense-phase zone and enhances the mixing and movement of materials by improving the intensity of turbulence. In addition, the involvement of secondary air adjusts and maintains the bed temperature, ensuring that the combustor operates in a steady state.

Fig. 4a and b illustrates the bed temperatures under different air split ratios with the tobacco stem feeding rates at 9 kg/h and 10 kg/h, respectively. With the increasing secondary air ratio, the maximum bed temperature in the dense phase zone also increases, but the temperature of the combustor along the dilute-phase zone decreases as a result. In addition, it can be observed from Table 4 that, as the secondary air ratio increased, the CO concentration in stack gas tends to decrease. This is because the volatiles escape rapidly from the dense-phase zone after heating, and the excessive oxygen provided by the secondary air could make these volatiles burn completely; with more heat generated, less CO is emitted.

From the discussions above, it is evident that the effects of secondary air to the combustion lies in two aspects. First, the secondary air increases the oxygen concentration in the dilute-phase zone, which is beneficial to the overall combustion efficiency and reducing the emission of pollutants. Second, excessive secondary air decreases the temperature in the dilute-phase zone, preventing the volatiles from burning out and, thus, more CO, CH_4 and other organic pollutants such as polycyclic aromatic hydrocarbons (PAHs) are emitted in the flue gas. Considering these effects, in order to keep the combustor operating at a normal temperature, the air split ratio between primary air and secondary air must be reasonably set. Under experimental conditions, the bed temperature is considerably high and less CO is emitted when the split ratio of primary air to secondary air is set at 1:1.36.

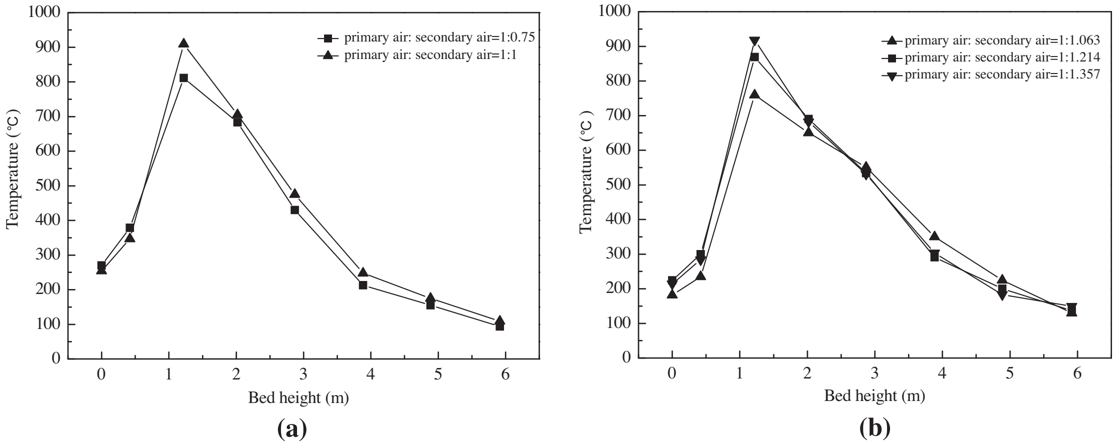

Fig. 4. The effect of air split ratio on the bed temperature profile under different feeding rates. (a) Bed temperature distribution under feeding rate of 9 kg/h; (b) bed temperature distribution under feeding rate of 10 kg/h.

3.3. Bed material agglomeration

3.3.1. Bed material agglomeration phenomenon

Biomass ashes are usually dominated by silicon, calcium and potassium, which are the main components that cause bed agglomeration and ash sintering (Bartels et al., 2008). From the data obtained during XRF analysis in Table 5, it can be seen that the K_2O and CaO contents are quite high. These contents may significantly contribute to the deposition and bed agglomeration problems in the combustion of biomass.

The silica sand underwent agglomeration under normal combustion temperature in approximately 1 h operation time when the pressure drop fluctuated markedly. Photographs of the agglomeration material are shown in Fig. S5a–c. It can be observed that, when using silica sand as bed material, the combustion of tobacco stem leads to serious agglomeration, and a large amount of agglomeration material was adhered to the inner wall of the combustor, which reduced the diameter of the column significantly. The agglomerates discharged from the bed appeared to be solid and difficult to be broken into smaller parts.

On the contrary, when using cinder as a bed material under normal operation temperatures, no apparent agglomeration was observed and the bed temperature and pressure drop did not vary erratically during the combustion process. After the experiments were completed, no sticky agglomeration material was found on the inner wall of the combustor; however, a small amount of deposition slices, with thickness of 1–2 mm, was found, as shown in Fig. S5c. The bed material discharged from the bottom of the combustor was observed to evaluate the extent of agglomeration. The cinder discharged from the combustor was sieved and the result showed that the weight percentages of particles with different size ranges of 3, 2–3 and 1–2 and <1 mm were 0.7%, 1.7%, 41.5% and 56.1%, respectively. Thus, the cinder did not agglomerate during tobacco stem combustion.

3.3.2. Agglomeration characteristics

As shown in Table 5, the components of tobacco stem ash, raw bed materials and agglomeration materials were analysed by X-ray fluorescence (XRF, EAGLE III).

It was observed that the contents of Si, K, Ca and Cl in ash components of tobacco stem were very high, which contributed to bed agglomeration in FB. In addition, significant changes on the components of bed materials occurred after the experiments were completed. After continuous operation, alkali metals and alkali earth metals such as potassium and calcium accumulated notably in the silica sand, although these elements are scarcely present in raw silica sand. However, the contents of silicon and alumina decreased significantly, suggesting that the agglomeration is mainly caused by the accumulation of alkali metal compounds in the ash of tobacco stem during the combustion. The potassium compounds can be converted to compounds with low melting point such as $K_2S_2O_7$ (325 °C) and KCl (770 °C) (Elisabet et al., 2005; Olofsson et al., 2002) as temperature increases, and these compounds bond the bed material particles together because of their strong adhesiveness. Furthermore, potassium elements can migrate from the ash and combine with SiO_2 in silica sand to form eutectic compounds with low melting point, such as $K_2O{\cdot}2SiO_2$ and $K_2Si_4O_9$ (Elisabet et al., 2005; Olofsson et al., 2002). As the amount of eutectic compounds continue to grow, the bed material becomes stickier and the particles need more momentum to overcome the sticky resistance caused by the sticky bed material in the bed. Although the components of alkali metals have also aggregated in cinder, the movement is much smoother than that on a bed of silica sand. Also, the contents of iron increase notably when cinder is used, which indicates that the deposition slices obtained in the combustor do not comprise compounds with low melting point and is unlikely to cause agglomeration during prolonged processing.

The surface morphology of both initial bed materials and agglomerates obtained after combustion was studied by scanning

Table 5
Chemical compositions of tobacco stems, bed materials and agglomerates wt.%.

Components	Na_2O	MgO	Al_2O_3	SiO_2	P_2O_5	K_2O	CaO	TiO_2	Fe_2O_3	SO_3	Cl
Tobacco stem	0.38	5.88	5.00	16.04	4.05	21.20	31.36	0.04	0.08	7.96	8.34
Raw silica sand	NA	NA	2.20	97.71	NA	NA	NA	NA	NA	NA	NA
Silica sand agglomerates	2.28	5.09	1.37	4.95	3.4	22.08	36.61	0.20	0.26	12.33	10.85
Raw cinder	0.83	0.72	18.97	73.34	0.57	0.71	0.36	0.57	1.85	1.30	0.77
Cinder slices	1.29	0.1	2.78	79.34	1.19	1.12	0.81	0.38	7.73	1.80	6.73

Note: NA represents the undetected chemical components.

Table 6
EDX analysis results of agglomerates wt.%.

Component	Mg	Al	Si	P	S	K	Ca	Fe	Cl
Silica sand	4.47	5.79	8.03	2.45	3.74	27.39	39.04	NA	9.09
Cinder	0.2	0.81	49.84	NA	2.05	3.46	0.75	42.89	NA

Note: NA represents the undetected chemical components.

electronic microscopy (SEM) using Quanta 200 microscope coupled with dispersive X-ray spectrometer (EDX, The FEI Company, The Netherlands). The main parameters were set as follows: WD was 12.9 mm, HV was set at 20.0 kV, magnification was ranged from 300 to 2400, and Spot was 3.5. The results are shown in Fig. S6. It can be observed that the morphology of the bed materials have changed significantly after combustion. Most of silica sand particles were coated by a tight structure of fine particles; however, the cinder slice has a porous structure and some fusion compounds were observed on the surface of the particles, but very little amount of fine particles are attached to the surface of the particle. This indicates that a sticky layer is formed on the outside surface of the bed material particles with different structure, and the structure varies among various species of bed materials (Bapat et al., 1997).

The results of EDX analysis on the bed material particles, shown in Table 6, indicate that elements such as K, Ca, Mg, and Cl accumulated enormously on the surface of the silica sand particle, and a strong enrichment of iron and silicon on the surface of the cinder particle is observed. It is interesting to find that the surface of the silica agglomerates has the chemical composition similar to that of the original ash, while the cinder bed material does not. This result indicates that the mineral elements in the fuel ash exhibit different patterns of movement during combustion with different bed materials. One possible reason for the bed agglomeration can be elaborated as follows: the bed material particles adhere to fine ash particles during random collisions and attritions with ash particles; as the adhesion proceeds, a sticky ash-related layer was formed on the surface of the bed material particles. As the temperature grows, the chemical reaction between the ash layer and bed material becomes more drastic. The silica can combine with potassium and calcium to form a ternary system K_2O–CaO–SiO_2 through alkali–silicon reaction (Scala and Chirone, 2006). The molten compounds in this system also contribute considerably to agglomeration. And such compounds continue to accumulate and become more viscous when temperature increases, which causes more particles to stick together and increases the sticky resistance at the same time. When the sticky resistance outweighs the momentum supplied by fluidized air, defluidization occurs.

The alumina and iron compounds in cinder can react with alkali metal to form compounds with high melting point (Acharya, 1997; Olofsson et al., 2002; Shimizu et al., 2006):

$$X_2O + Fe_2O_3 \rightarrow X_2Fe_2O_4 \tag{9}$$

$$X_2CO_3 + Fe_2O_3 \rightarrow X_2Fe_2O_4 + CO_2 \tag{10}$$

$$X_2O + Al_2O_3 \rightarrow X_2Al_2O_4 \tag{11}$$

$$X_2CO_3 + Al_2O_3 \rightarrow X_2Al_2O_4 + CO_2 \tag{12}$$

$$X_2O \cdot nSiO_2 + Fe_2O_3 \rightarrow X_2O \cdot Fe_2O_3 \cdot nSiO_2 \tag{13}$$

$$X_2O \cdot nSiO_2 + Al_2O_3 \rightarrow X_2O \cdot Al_2O_3 \cdot nSiO_2 \tag{14}$$

$$X_2O \cdot nSiO_2 + Al_2O_3 \rightarrow X_2O \cdot Al_2O_3 \cdot (n-1)SiO_2 + SiO_2 \tag{15}$$

where, X represents the alkali metal elements.

Such high melting compounds can prevent the alkali metal from converting and migrating to low-melting point compounds, and thus, inhibit the bed agglomeration to some extent.

To further investigate the effect of high temperature on bed agglomeration, a test of combustion of cinder and tobacco stem mixture under the mixing ratio 1:1 was conducted in a Muffle furnace at 900 °C. The deposit obtained after the combustion was sampled and analysed by X-ray diffraction (XRD, PANalytical B.V., X'Pert PRO, The Netherlands). The results indicate that in addition to silica and $CaSO_4$, the mixture contained some complex crystalline compounds such as $3Al_2O_3 \cdot 2SiO_2$, $3Na_2O \cdot 2Al_2O_3 \cdot 4SiO_2$ and $Na_3K_3Al_6Si_6O_{24}$, the melting points of which were relatively high, i.e. the compounds are not easy to agglomerate (Olofsson et al., 2002). The results, in turn, indicate that the iron and alumina compounds in cinder can combine with alkali metal compounds through chemical reactions to form compounds with high melting point as described in Eqs. (11)–(15), thus, can be used to eliminate the bed agglomeration during combustion.

4. Conclusion

Tobacco stem is easy to ignite and the combustion process can be set up into four separate steps. The tobacco stem burns steadily in the FB and a considerable fraction of heat is generated in the dense zone below the feeder port. Adding a suitable amount of secondary air improves the combustion efficiency and decreases the emission of pollutants. Silica sand is not suitable as a bed material in tobacco stem combustion because of its high content of silica. However, the alumina and iron content in cinder can significantly eliminate agglomeration problems during combustion significantly.

Acknowledgements

The authors wish to express the great appreciation of the financial support from National Nature Science Foundation of China (50930006 and 51021065) and National Technology Support Program (2011BAD15B05). The authors also wish to express the great appreciation of the technical support from Analytical and Testing Centre in Huazhong University of Science & Technology (http://atc.hust.edu.cn). Mr. Ho Simon Wang, at HUST Academic Writing Centre, and Mr. Yingquan Chen, at HUST SKLCC, have helped improve the presentation of the manuscript.

Appendix A. Supplementary data

Supplementary data associated with this article can be found, in the online version, at doi:10.1016/j.biortech.2011.12.119.

References

Acharya, P., 1997. Process challenges and evaluation of bed agglomeration in a circulating bed combustion system incinerating red water. Environ. Prog. 16 (1), 54–64.

Andreae, M.. 1991. Biomass burning – its history, use, and distribution and its impact on environmental quality and global climate. Global biomass burning-Atmospheric, climatic, and biospheric implications (A 92–37626 15–42). MIT Press, Cambridge, MA, 1991.

Bapat, Kulkarni, Bhandarkar, 1997. Design and operating experience on fluidized bed boiler burning biomass fuels with high alkali ash. In: The 14th International Conference on Fluidized Bed Combustion, Vancouver, New York, pp. 165–174.

Barrena, R., Vazquez, F., Sanchez, A., 2008. Dehydrogenase activity as a method for monitoring the composting process. Bioresource Technol. 99 (4), 905–908.

Bartels, M., Lin, W., Nijenhuis, J., 2008. Agglomeration in fluidized beds at high temperatures: mechanisms, detection and prevention. Prog. Energ. Combust. 34 (5), 633–666.

Brus, E., Hman, M., Nordin, A., Bostrm, D., Hedman, H., Eklund, A., 2004. Bed agglomeration characteristics of biomass fuels using blast-furnace slag as bed material. Energy Fuels 18 (4), 1187–1193.

Castron, R.C., Agrupis, S.C., 2000. Study on the manufacturing fiber board with tobacco stems. J. Tobacco Sci. Technol. 23 (7), 15–16 (in Chinese).

Chirone, R., Salatino, P., Scala, F., 2008. Fluidized bed combustion of pelletized biomass and waste-derived fuels. Combust. Flame 155 (1–2), 21–36.

Elisabet, B., Marcus, O., Anders, N., 2005. Mechanisms of bed agglomeration during fluidized-bed combustion of biomass fuels. Energ. Fuel. 19 (3), 825–832.

Fang, M., Yang, L., Chen, G., Shi, Z., Luo, Z., Cen, K., 2004. Experimental study on rice husk combustion in a circulating fluidized bed. Fuel Process. Technol. 85 (11), 1273–1282.

Gil, M.V., Casal, D., Pevida, C., 2010a. Thermal behaviour and kinetics of coal/biomass blends during co-combustion. Bioresource Technol. 101 (14), 5601–5608.

Gil, M.V., Oulego, P., Casal, M.D., Pevida, C., Pis, J.J., Rubiera, F., 2010b. Mechanical durability and combustion characteristics of pellets from biomass blends. Bioresource Technol. 101 (22), 8859–8867.

Gogebakan, Z., Gogebakan, Y., Selçuk, N., Selçuk, E., 2009. Investigation of ash deposition in a pilot-scale fluidized bed combustor co-firing biomass with lignite. Bioresource Technol. 100 (2), 1033–1036.

Hurt, R.H., Gibbins, J.R., 1995. Residual carbon from pulverized coal fired boilers: 1. Size distribution and combustion reactivity. Fuel 74 (4), 471–480.

Kouprianov, V.I., Permchart, W., 2003. Emissions from a conical FBC fired with a biomass fuel. Appl. Energ. 74 (3–4), 383–392.

Li, J., Li, J.C., Wu, X.H., 2010. The study on utilization of tobacco waste. J. Yunnan Chem. Technol. 37 (2), 44–49 (in Chinese).

Li, W., Zhang, L., Peng, J., Li, N., Zhang, S., Guo, S., 2008. Effects of microwave irradiation on the basic properties of woodceramics made from carbonized tobacco stems impregnated with phenolic resin. Ind. Crops Prod. 28 (2), 143–154.

Li, X.G., Lv, Y., Ma, B.G., 2011. Thermogravimetric investigation on co-combustion characteristics of tobacco residue and high-ash anthracite coal. Bioresource Technol. 102 (20), 9783–9787.

Li, Z., Zhao, W., Li, R., Wang, Z., Li, Y., Zhao, G., 2009. Combustion characteristics and NO formation for biomass blends in a 35-ton-per-hour travelling grate utility boiler. Bioresource Technol. 100 (7), 2278–2283.

Lu, X., 2000. The study on the electrochemical synthesis of nicotinic acid with nicotine. J. Fine Chem. 17 (8), 453–455 (in Chinese).

Olofsson, G., Ye, Z.C., Bjerle, I., 2002. Bed agglomeration problems in fluidized-bed biomass combustion. Ind. Eng. Chem. Res. 41 (12), 2888–2894.

Piotrowska-Cyplik, A., Olejnik, A., Cyplik, P., Dach, J., Czarnecki, Z., 2009. The kinetics of nicotine degradation, enzyme activities and genotoxic potential in the characterization of tobacco waste composting. Bioresource Technol. 100 (21), 5037–5044.

Quadrelli, R., Peterson, S., 2007. The energy-climate challenge: recent trends in CO_2 emissions from fuel combustion. Energy Policy 35 (11), 5938–5952.

Scala, F., Chirone, R., 2006. Characterization and early detection of bed agglomeration during the fluidized bed combustion of olive husk. Energy Fuels 20 (1), 120–132.

Shimizu, T., Han, J., Choi, S., Kim, L., Kim, H., 2006. Fluidized-bed combustion characteristics of cedar pellets by using an alternative bed material. Energy Fuels 20 (6), 2737–2742.

Sung, Y.J., Seo, Y.B., 2009. Thermogravimetric study on stem biomass of Nicotiana tabacum. Thermochim. Acta 486 (1–2), 1–4.

Tarelho, L.A.C., Neves, D.S.F., Matos, M.A.A., 2011. Forest biomass waste combustion in a pilot-scale bubbling fluidised bed combustor. Biomass Bioenerg. 35 (4), 1511–1523.

Valverde, J.L., Curbelo, C., Mayo, O., 2000. Pyrolysis kinetics of tobacco dust. Chem. Eng. Res. Des. 78 (6), 921–924.

Varhegyi, G., Antal, M.J., Jakab, E., 1997. Kinetic modeling of biomass pyrolysis. J. Anal. Appl. Pyrolysis 42 (1), 73–87.

Wang, C., Wang, F., Yang, Q., 2009. Thermogravimetric studies of the behavior of wheat straw with added coal during combustion. Biomass Bioenerg. 33 (1), 50–56.

Wang, W., Wang, Y., Yang, L., 2005. Studies on thermal behavior of reconstituted tobacco sheet. Thermochim. Acta 437 (1–2), 7–11.

Xu, Z.H., Wang, N.R., Cui, Y., 2000. Innovation for energy saving of flue-curing barn. J. Anhui Agric. Sci. 28 (6), 795–798 (in Chinese).

Yang, H., Yan, R., Chin, T., Liang, D.T., Chen, H., Zheng, C., 2004. Thermogravimetric analysis-Fourier transform infrared analysis of palm oil waste pyrolysis. Energy Fuels 18 (6), 1814–1821.

Zhong, W., Zhu, C., Shu, M., Sun, K., Zhao, L., Wang, C., Ye, Z., Chen, J., 2010. Degradation of nicotine in tobacco waste extract by newly isolated *Pseudomonas* sp. ZUTSKD. Bioresource Technol. 101 (18), 6935–6941.